ELSEVIER

Journal of Structural Geology 29 (2007) 385–395

JOURNAL OF STRUCTURAL GEOLOGY

www.elsevier.com/locate/jsg

Fracture-controlled fluid circulation and dissolutional weathering in sinkhole-prone carbonate rocks from central Italy

Andrea Billi [a,*], Andrea Valle [a], Mauro Brilli [b], Claudio Faccenna [a], Renato Funiciello [a]

[a] *Dipartimento di Scienze Geologiche, Università ''Roma Tre'', Largo S. L. Murialdo, 1, 00146 Rome, Italy*
[b] *Istituto di Geologia Ambientale e Geoingegneria, CNR, Rome, Italy*

Received 21 June 2006; received in revised form 22 September 2006; accepted 22 September 2006
Available online 2 November 2006

Abstract

Fractures, karstic cavities, and calcite precipitates are analysed on Mesozoic, carbonate strata from the Cornicolani Mountains, central Italy, to quantify the relationships between fractures and related karstic cavities and to infer the fracture-controlled fluid pathways. The study area is characterized by active sinkholes and other karstic caves, which are among the deepest ones in the world. Results show a clear control of fractures on the process of dissolutional weathering and, therefore, on the fluid circulation. A model is proposed, in which two different modes of dissolutional weathering coexist: (i) a mode of diffuse weathering consisting in the dissolutional enlargement of closely spaced joints and bedding surfaces. This process affects the strata situated at depths of up to 5 m; (ii) a mode of more concentrated weathering active along highly permeable fault damage zones at depths of at least 70 m. These processes are mostly connected with the shallow circulation of calcite-dissolving meteoric waters, and are controlled by the disparity of permeability between the fault damage zones and the surrounding jointed strata. Some calcite precipitates along the studied fault damage zones may be connected with a dissolutional process operated by waters that interacted with the adjacent quiescent volcanic district. Such calcite-dissolving waters and the presence of high-permeable fault damage zones, along which the waters may ascent, are probably the cause for the development of some of the deep sinkholes along faults in the study area.

Keywords: Joint; Fault; Fluid; Sinkhole; Stable isotope; Weathering

1. Introduction

Fractures in carbonate rocks have long been recognised as major features controlling fluid circulation and related karstic processes, particularly in the early phases of karstification (Swinnerton, 1932; Sweeting, 1950; Fetter, 1980; Ford and Ewers, 1978; White, 1988; Palmer, 1991). Several numerical models have been developed to infer the relationships between rock fractures, fluid circulation and karstic processes (e.g. Gabrovšek and Dreybrodt, 2001; Kaufmann, 2002, 2003a; Gabrovšek et al., 2004; Romanov et al., 2003; Andre and Rajaram, 2005). The equilibrium chemistry of the limestone and dolostone dissolution has been suitably defined, and there are formal models for the kinetics of dissolution. Such models have been used to predict the fracture enlargement by fluid circulation in karstic environments (e.g. Dreybrodt, 1988; White, 1988, 2002; Ford and Williams, 1989). Despite the numerous predictive models, the small number of field-based quantitative studies on the relationship between fractures and karstic structures (e.g. Rodet, 1999) significantly restrains a full comprehension of fracture-controlled fluid circulation and relative karstification at both epigeal and hypogeal levels.

The aim of this paper is to contribute to the knowledge of fracture-controlled fluid circulation and relative karstic processes at epigeal and hypogeal levels in carbonate rocks. The relationship between fractures and karstic structures (i.e. cavities) is quantitatively addressed by considering a set of field data collected from Mesozoic carbonate strata exposed in the Cornicolani Mountains, central Italy (Fig. 1). Results from stable isotope analyses done on calcite concretions

* Corresponding author. Tel.: +39 0654888016; fax: +39 0654888201.
E-mail address: billi@uniroma3.it (A. Billi).

0191-8141/$ - see front matter © 2006 Elsevier Ltd. All rights reserved.
doi:10.1016/j.jsg.2006.09.008

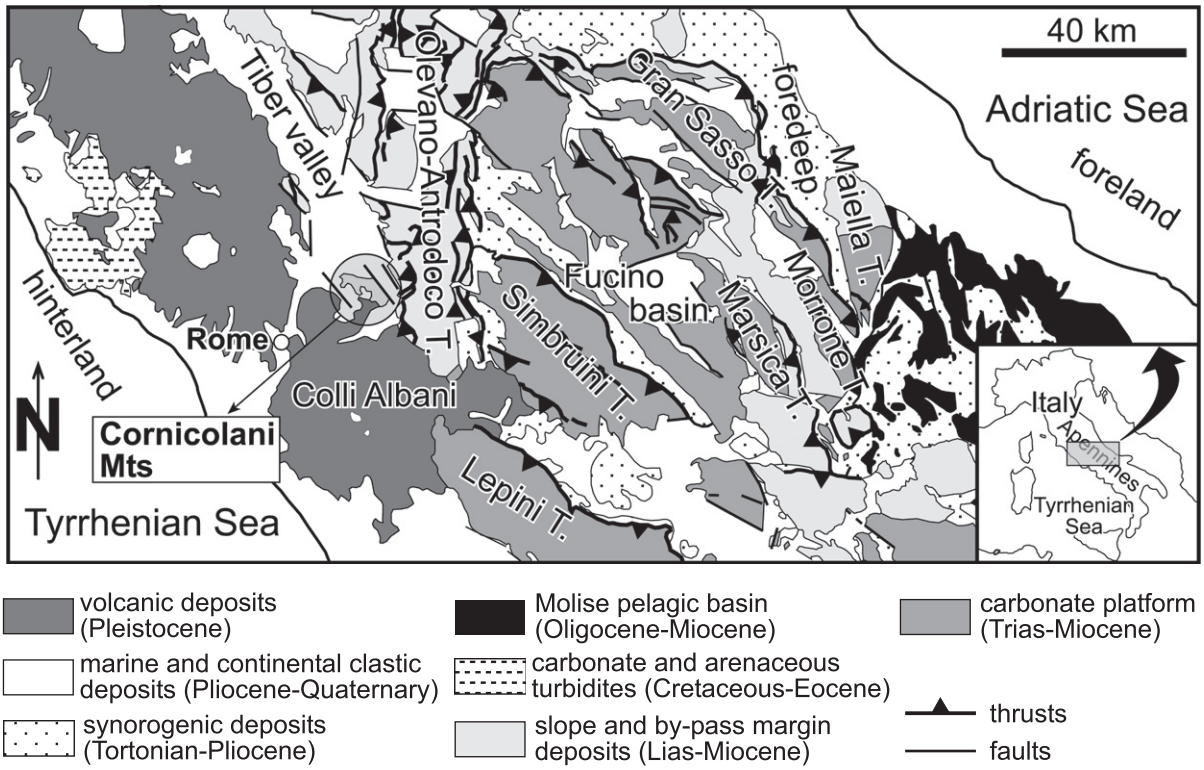

Fig. 1. Geological setting of the central Apennine fold-thrust belt, Italy. The Cornicolani Mountains are located about 30 km in the northeast of Rome. T = thrust sheet.

exposed along some faults are included to understand the provenance of calcite-dissolving fluids. Results from this study provide an insight into the formation of karstic sinkholes (Fig. 2), which, in this region, have frequently developed during recent and historical times (Faccenna et al., 1993; Salvati and Sasowsky, 2002). Such results may therefore be useful to mitigate sinkhole-related hazards (e.g. Sowers, 1996). The same results may also serve as input data in numerical models of karst aquifer evolution (e.g. Dreybrodt, 1996; Clemens et al., 1999; Kaufmann and Braun, 1999, 2000; Bauer et al., 2000; Gabrovšek, 2000; Gabrovšek and Dreybrodt, 2001; Romanov et al., 2003).

2. Geological setting

The Cornicolani Mountains are located in the central Apennine fold-thrust belt (or Apennines, Fig. 1). This belt developed within the frame of convergence between the African and Eurasian plates and grew by deforming the Mesozoic–Cenozoic sedimentary cover of the Adriatic foreland during the Neogene (Malinverno and Ryan, 1986; Dewey et al., 1989). Through time, the contractional deformations migrated toward the east, mostly in a piggyback forelandward sequence (Patacca et al., 1992; Cipollari and Cosentino, 1995) favoured by the parallel retreat of the subduction zone toward the Adriatic foreland (Malinverno and Ryan, 1986).

The Cornicolani Mountains (Fig. 2) are part of the N-striking, E-verging Olevano-Antrodoco thrust system (Figs. 1 and 2), which developed in-sequence during early Messinian time and reactivated out-of-sequence in late Messinian–early Pliocene time (Cipollari and Cosentino, 1991; Cavinato and DeCelles, 1999). In the Cornicolani Mountains, the Messinian–Pliocene thrusts have been later (Pliocene-Quaternary times) disrupted by N-striking, right-lateral, strike-slip faults (Faccenna and Funiciello, 1993; Faccenna et al., 1994). In the south of the Cornicolani Mountains, these strike-slip faults have formed a pull-apart basin (i.e. the Acque Albule Basin, Fig. 2), which is filled by Quaternary marine and continental sediments and by more than 80 m of travertine deposits, with a maximum age of about 165 ka (Faccenna et al., 1994). In the Acque Albule Basin (Fig. 2a), sinkholes, thermal anomalies, hot springs, and gas (i.e. mostly CO_2 and H_2S) vents are approximately aligned along the southern prolongation of the N-striking, strike-slip faults exposed in the Cornicolani Mountains (Maiorani et al., 1992; Minissale et al., 2002). The occurrence of hot springs and gas vents in the Acque Albule Basin is connected with the adjacent volcanic district (i.e. Colli Albani, Fig. 1), which is presently quiescent (Funiciello et al., 2003).

In the Cornicolani Mountains and surrounding areas, several sinkholes and karstic caves occur (Fig. 2a). In the western sector of the Cornicolani Mountains, Pozzo del Merro is the deepest flooded sinkhole presently known in the world (Caramanna, 2002; Knab, 2003; Gary et al., 2003). In 2002, this sinkhole was explored with a remotely operated vehicle that detected the base of the sinkhole at a depth of 392 m from its superficial rim, the height of which is about 130 m a.s.l. The hypogeal karst processes in the Cornicolani Mountains and adjacent areas are ongoing as demonstrated by the sudden

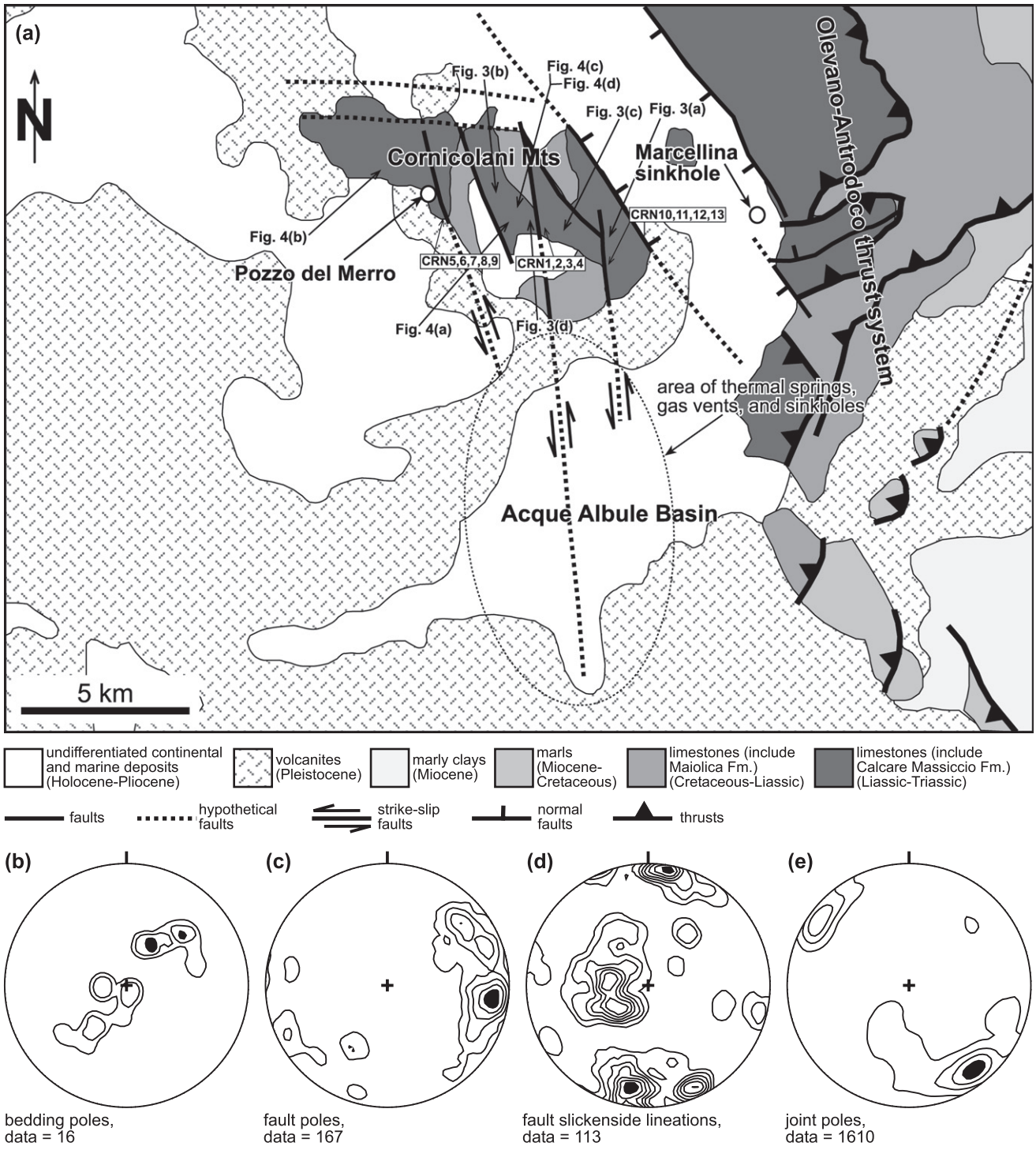

Fig. 2. (a) Geological map of the Cornicolani Mountains and adjacent areas. Locations of photographs and samples discussed in the text are shown. (b–e) Lower hemisphere, equal-area plots showing density contours to bedding poles, fault poles, fault slickenside lineations, and joint poles, respectively. Black filling corresponds to the maximum density. The structural data were collected in 47 sites located in the carbonate formations of the Cornicolani Mountains.

formation, in February 2001, of the Marcellina sinkhole (diameter ≈70 m, depth ≈20 m; Colombi, 2002) located about 3 km in the east of the Cornicolani Mountains (Fig. 2a).

The thrust sheets forming the central Apennines mostly consist of shallow-water marine carbonates and deep-water limestones with lime resediments. In the Cornicolani Mountains (Fig. 2a), two major carbonate formations are exposed (Chiocchini et al., 1979; Cosentino et al., 2004): the Calcare Massiccio Formation (Hettangian–Sinemurian) and the Maiolica Formation (Tithonian–Barremian). The Calcare Massiccio Formation consists of platform limestones with a mud-supported grainstone texture and, in places, with a micrite matrix. The

limestone forming the Calcare Massiccio Formation is poorly stratified or massive. The base and thickness of the Calcare Massiccio Formation in the Cornicolani Mountains are unknown, but, in the central Apennines, the thickness of this formation is inferred as being about 800 m (i.e. after well logs). The Maiolica Formation consists of a pelagic micritic limestone arranged in beds between ~10 and ~50 cm in thickness. This limestone is often dolomitized. The thickness of the Maiolica Formation in the Cornicolani Mountains is about 30 m (Cosentino et al., 2004). Both the Calcare Massiccio Formation and the Maiolica Formation consist of a very compact limestone whose matrix permeability is low and negligible for the aims of this paper. The primary porosity for the most compact facies of these formations is, in fact, less than about 0.5–1% (Passeri, 1972). Pathways for fluid circulation through the Calcare Massiccio and Maiolica formations are provided by fractures (i.e. faults and joints) and bedding surfaces (Alfonsi et al., 1991; Maiorani et al., 1992).

3. Methods and results

3.1. Fractures and karstic cavities

In the Cornicolani Mountains (Fig. 2a), bedding mainly includes NW-striking surfaces dipping either toward the northeast or toward the southwest (Fig. 2b). Faults are preferentially N10°-striking, high-angle (>60°) surfaces (Fig. 2c) characterized by dip-slip and strike-slip kinematic indicators (Fig. 2d), which show normal and right-lateral displacements, respectively. Faults are usually bounded by a narrow damage zone consisting of fractured limestone and coarse breccias. Layers of gouge and fine-grained cataclastic rocks are usually absent or rare along the studied faults. Joints mainly consist of closely spaced, N50°-striking, high-angle surfaces (Fig. 2e) with a perpendicular aperture between 0.01 and 1 cm. Attitude and aperture of joints are kinematically consistent with the N10°-striking, right-lateral faults (Alfonsi et al., 1991; Faccenna and Funiciello, 1993; Faccenna et al., 1994).

Joints observed in natural exposures in the Cornicolani Mountains are strongly karstified (i.e. widened by dissolution) both in the Calcare Massiccio Formation and in the Maiolica Formation (Fig. 3). Karstic cavities preferentially occur along joints and bedding surfaces. Where two or more joints intersect, the karstic cavities are elongated along all joints, thus assuming L-, S-, T-, X-, Y-, Z-, or +-like shapes in cross-section (Fig. 3). In man-made exposures (i.e. within active or recently closed quarries), we observed that the effects of the dissolutional weathering of joints and bedding surfaces occur only in the shallow strata, i.e. less than about 5 m below the surface. At these depths, karstic caves as large as a few metres or decametres are widespread (e.g. Fig. 4a). Such caves are usually filled by breccias. At deeper levels (i.e. at depths greater than about 5 m), the effects of the dissolutional weathering on joints and bedding surfaces decrease and are absent at depths greater than about 10 m (Fig. 4b). An exception is constituted by the damage zones surrounding some high-angle faults that cut through the studied carbonate strata (Fig. 4c). Along these zones, karstic cavities and calcite concretions (Fig. 4d) are frequent even at depths greater than 20 m from the fieldsurface (i.e. up to a maximum available depth of about 70 m).

To examine the geometrical relationship between joints and related karstic cavities, we analysed in detail 10 exposures of limestone located at depths between 0 and 1 m from the fieldsurface, six in the Calcare Massiccio Formation and four in the Maiolica Formation. The analysed exposures are approximately perpendicular to the major set of joints. In each exposure, we measured the azimuth of joints and the azimuth of the long axis (i.e. as determined in cross-section) of the associated karstic cavities. Azimuths were measured from an arbitrarily set reference line using a protractor. The collected data consist of a total of 389 and 377 azimuths for the joints and for the long axis of the associated karstic cavities, respectively. For each exposure, the two populations of azimuths (one for the joints and one for the long axis of the associated karstic cavities) were fitted by a Gaussian equation (e.g. Salvini et al., 1999) and the relative mean values plotted in an appropriate diagram (Fig. 5a). The relative standard deviations (i.e. obtained from the Gaussian equations) are $\leq 11°$. Fig. 5a shows a linear correlation between the azimuth of joints and that of the associated karstic cavities. The attitude of the best fit line (i.e. dipping about 45° and approximately passing through the origin of axes) shows the parallelism between the joints and the associated karstic cavities.

We examined the relationship between the density of joints and that of associated karstic cavities in the same exposures where we measured their orientation. In each exposure, we determined the joint density by the circle-inventory method (Titley, 1976; Davis and Reynolds, 1996). In this method, the joint density is the summed length of all joints within a properly drawn inventory circle, divided by the area of the circle. The joint density is here expressed in cm^{-1}. In the same exposures and by using the same inventory circles used for computing the joint density, we determined the density of the karstic cavities as the summed area of all cavities within the inventory circle, divided by the area of the circle. This density is a dimensionless number equivalent to the rock porosity (i.e. induced by the karstification) as measured in a cross-section. The collected data consist of a total of 508 joints and 448 karstic cavities in the Calcare Massiccio Formation (Fig. 5b), and a total of 456 joints and 368 karstic cavities in the Maiolica Formation (Fig. 5c). Fig. 5b and c shows direct correlations between the density of joints and that of the associated karstic cavities. The correlation is approximately exponential for the Calcare Massiccio Formation and approximately logarithmic for the Maiolica Formation.

To examine the relationship between the density of karstic cavities and relative depth, we determined the density of the karstic cavities (i.e. as above-explained) in 18 exposures of fractured carbonate strata from the Calcare Massiccio Formation. The exposures lie at depths of up to 70 m from the fieldsurface. The collected data consist of a total of 1080 karstic cavities. Results show an inverse power law relationship between the density of the karstic cavities and the relative depth

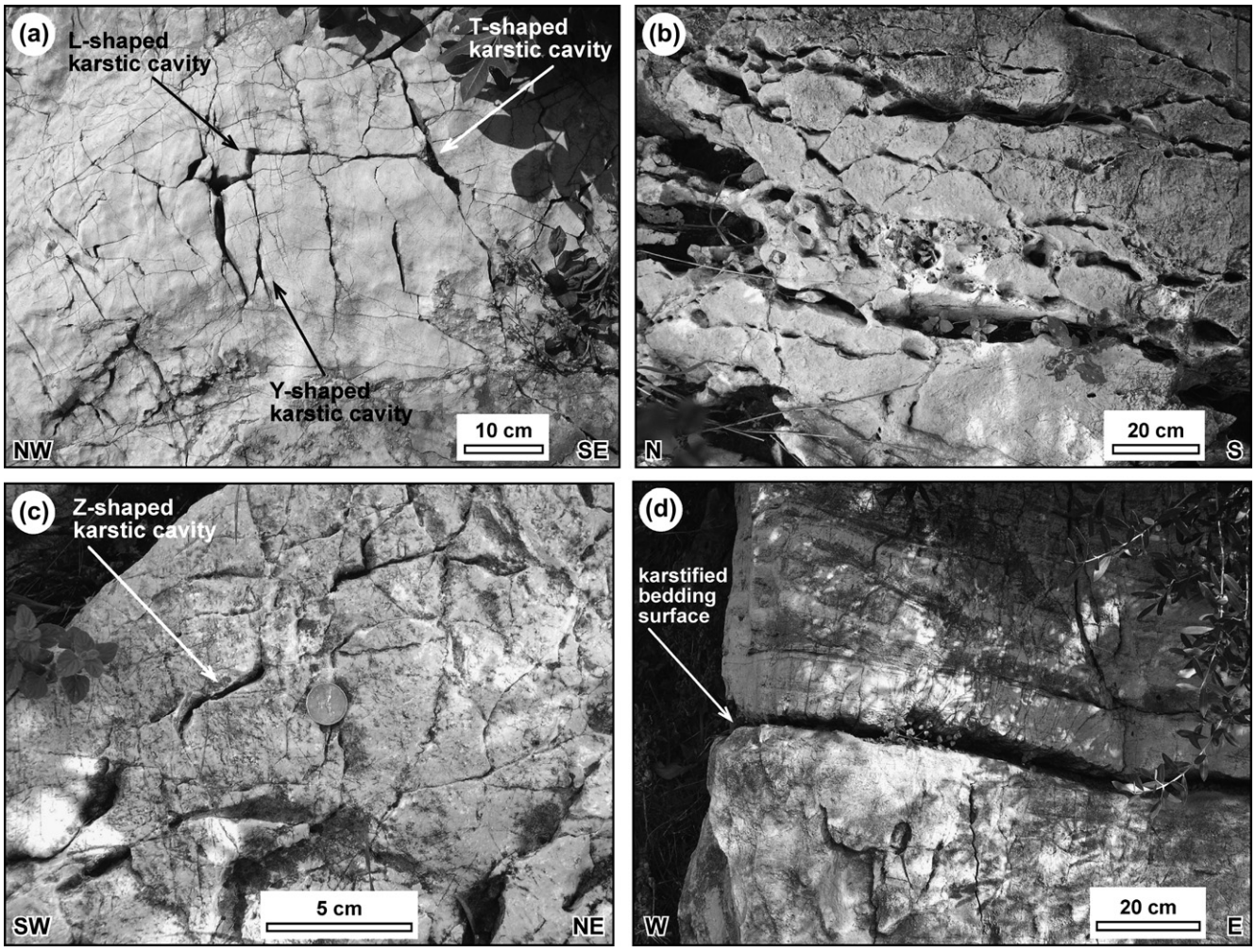

Fig. 3. (a–c) Photographs of karstified (i.e. dissolutionally weathered) joints within the carbonate strata of the Calcare Massiccio Formation. In (a) and (c), the karstic weathering is in an incipient or early phase, whereas in (d), such a process is in a more advanced phase. The karstic cavities are elongated and parallel (i.e. their long axis) to the joint attitude. (d) Photograph of a strongly karstified bedding surface within the carbonate rocks of the Calcare Massiccio Formation. Fig. 2 shows the locations of photographs.

(Fig. 5d). The density of the karstic cavities reduces to less than 2% for depths greater than 20 m.

3.2. Stable isotopes

A set of rock samples were collected at depths between ~30 and ~60 m from the fieldsurface along three strike-slip and transtensional faults exposed in the walls of active or recently closed quarries (Fig. 4c and d) in the Cornicolani Mountains (Table 1). The analysed faults have a damage zone consisting of coarse breccias and fractured carbonates that occupy a fault-perpendicular thickness of less than about 2–3 m across both the footwall and the hangingwall. Twelve samples are from calcite concretions deposited along the fault surfaces or within the associated damage zone (i.e. within the fault breccia, Fig. 4d), whereas 13 samples are from the fault host rocks (i.e. Calcare Massiccio Formation, Table 1). In each sample, the carbon and oxygen isotopes were analysed by using a Finnigan Mat 252 mass spectrometer and a Finnigan Kiel II instrument for the CO_2 extraction from the $CaCO_3$. Results are expressed in the usual δ-notation, where the reference standards are PDB (i.e. Pee Dee Belemnite) for carbon and SMOW (i.e. Standard Mean Oceanic Water) for oxygen.

Results from the stable isotope analyses are presented in Fig. 6, which shows two groups of data. The group referring to the calcite concretions is characterized by isotope compositions between 24.8‰ and 26.3‰ (vs. SMOW) for oxygen, and between −3.5‰ and −10.9‰ (vs. PDB) for carbon. The group referring to the host rock is characterized by isotope compositions between 28.3‰ and 29.7‰ (vs. SMOW) for oxygen, and between 1.2‰ and 3.0‰ (vs. PDB) for carbon.

4. Discussion

The data presented here show a clear structural control on the development of epigeal karstic structures and, therefore, on the fluid circulation through the studied carbonate strata. The karstification of these strata occurs by means of calcite-dissolving fluids, which mainly circulate along joints, faults, and bedding surfaces (Figs. 3–5). The origin of

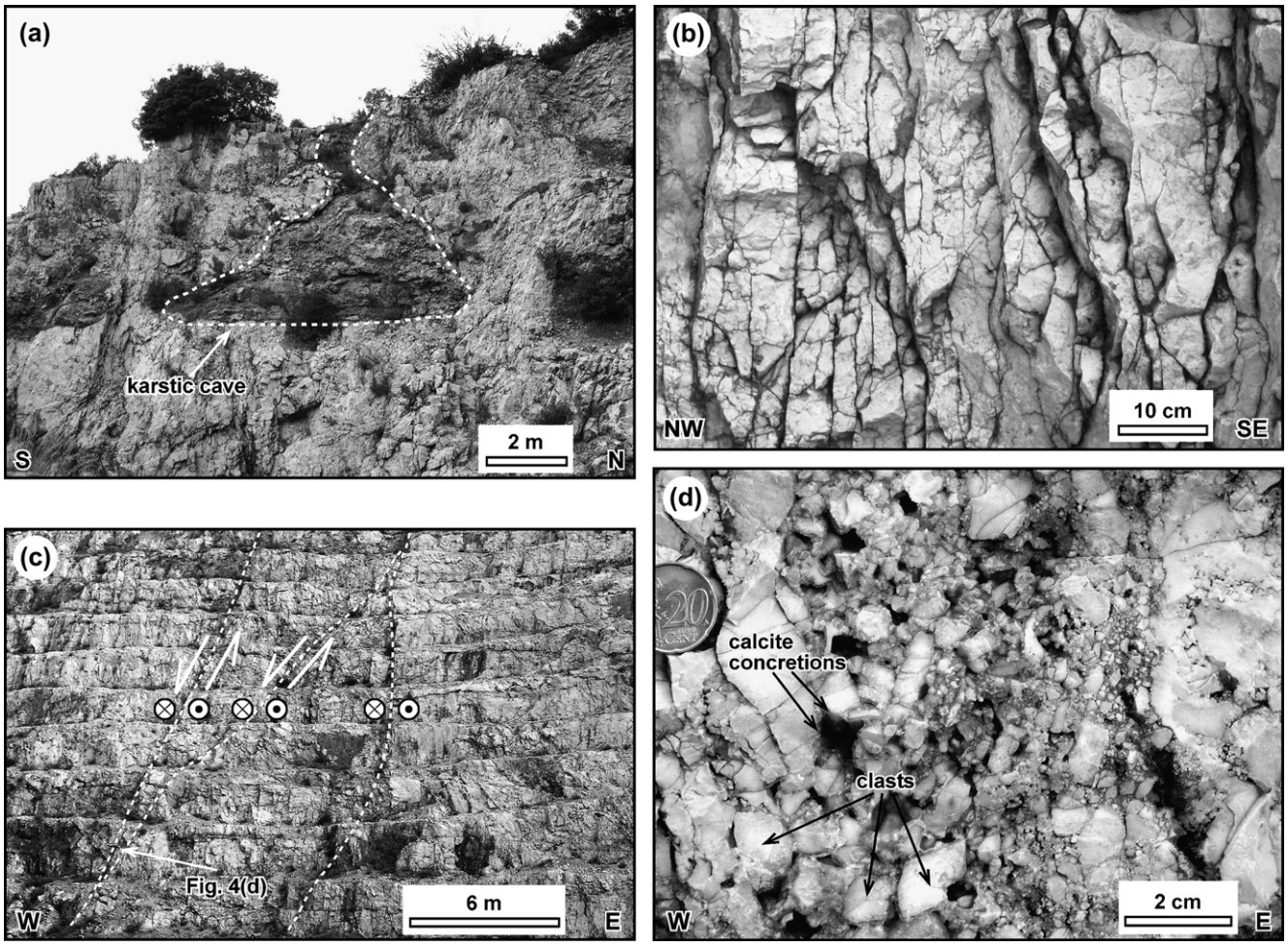

Fig. 4. (a) Photograph of a shallow (within about 6–8 m from the fieldsurface) karstic cave filled by a breccia consisting of carbonate clasts and a brownish matrix. The cave occurs within the carbonate strata of the Calcare Massiccio Formation. (b) Joints in carbonate rocks (Calcare Massiccio Formation) observed on a quarry wall at a depth of about 20 m from the fieldsurface. Note that the dissolutional weathering of joints is almost absent. (c) Artificial exposure (i.e. within a quarry) of fractured carbonate strata from the Calcare Massiccio Formation. Three strike-slip or transtensional faults cut across the entire exposure. (d) Detail from (c) showing a fault-related breccia impregnated by calcite concretions and affected by dissolutional weathering (i.e. the cavities). This exposure is at a depth of about 50 m from the fieldsurface. The calcite concretions were sampled for stable isotope analyses. See Fig. 2 for the locations of photographs.

calcite-dissolving fluids is inferred from the stable isotope analyses (Fig. 6). The isotope data for the host rocks (i.e. Calcare Massiccio Formation, Table 1) are typical of marine carbonate rocks (Veizer and Hoefs, 1976; for a comparison with further isotope data from the Calcare Massiccio Formation see Ghisetti et al., 2001). In contrast, the oxygen isotope data for the calcite concretions sampled along the faults and within the associated damage zones are consistent with calcite precipitates formed from water of meteoric origin at temperatures of less than about 20 °C. At these temperatures, the oxygen calcite-water fractionation is 29.5‰ vs. SMOW (O'Neil et al., 1969). This value, when combined with the average annual isotope composition of meteoric waters for the study area (i.e. about −5‰ vs. SMOW, Minissale et al., 2002 and references therein), is approximately consistent with the minimum $\delta^{18}O$ value measured in the samples analysed in this paper (i.e. 24.8‰ vs. SMOW, Table 1). The carbon isotope compositions for calcite concretions are significantly lower than those of the carbonate host rocks, these compositions showing the typical pattern of carbonate deposits in karstic environments (Schwarcz, 1986; Salomons and Mook, 1986; Gascoyne, 1992; McDermott, 2004), where organic carbon imprint is dominant. By assuming that only CO_2 from C_3 photosynthetic pathway vegetation type has been present in the Cornicolani Mountains area (since climatic conditions have not been warm or arid enough to support C_4 vegetation), the geochemical models indicate $\delta^{13}C$ of carbonate deposited from solution in the range of −14‰ to −6‰ vs. PDB (Hendy, 1971; Dreybrodt, 1980; Salomons and Mook, 1986). Excluding four samples, whose isotopic composition is slightly heavier (i.e. about −4‰ vs. PDB), most calcite concretions analysed in this paper fall into this interval (i.e. −14‰ to −6‰ vs. PDB, Table 1). Although $\delta^{13}C$-values greater than −6‰ vs. PDB might be consistent with a shallow provenance of the CO_2-bearing fluids (e.g. Baker et al., 1997), the occurrence, in the study area of a regional system of thermal spring waters and gas vents, mainly dominated by CO_2 derived from various crustal levels (Minissale et al., 1997) suggests a deeper CO_2

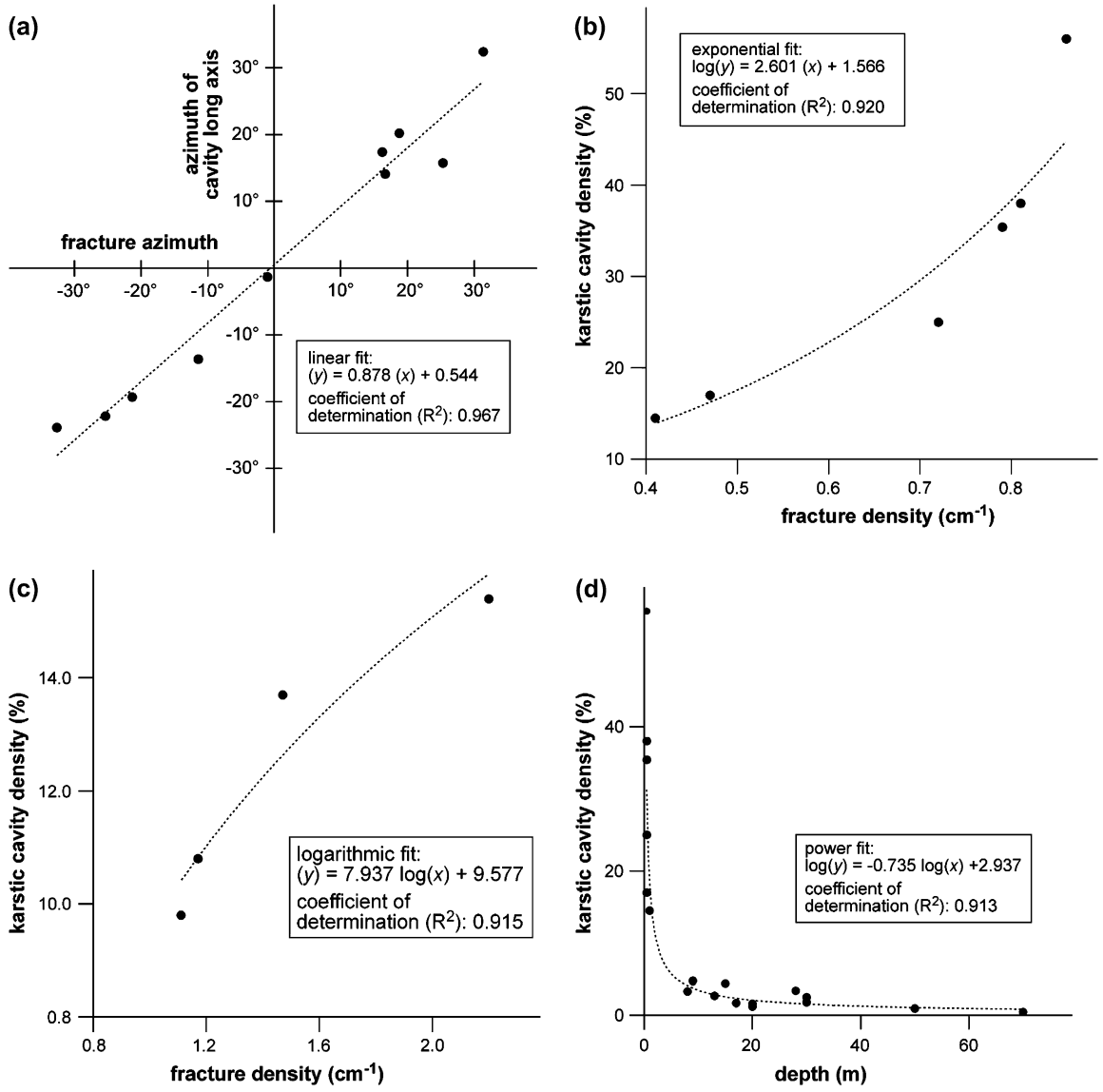

Fig. 5. (a) Relationship between the attitude of joints and the attitude of long axes of the associated karstic cavities. Positive values are for azimuthal angles taken clockwise from an arbitrarily set reference line, whereas negative values are for counter clockwise azimuthal angles. Each datum is representative of one exposure, over which several azimuth measurements were done. (b) Relationship between the density of joints and the density of the associated karstic cavities in carbonate strata from the Calcare Massiccio Formation. Each datum is representative of one exposure, over which the density measurements (i.e. for the joints and for the karstic cavities) were done. (c) Relationship between the density of joints and the density of the associated karstic cavities in carbonate strata from the Maiolica Formation. Each datum is representative of one exposure, over which the density measurements (i.e. for the joints and for the karstic cavities) were done. (d) Relationship between the density of karstic cavities and the depth of the relative exposure. Each datum is representative of one exposure, over which the measurement of density was done.

contribution in the development of the calcite concretions with δ^{13}C-values around $-4‰$ vs. PDB. In the geological framework of the Cornicolani Mountains, the most obvious source for such CO_2 is the adjacent quiescent volcanic district (i.e. Colli Albani, Fig. 1; see also Maiorani et al., 1992; Minissale et al., 1997).

The structural and isotope data presented in this paper can be fitted in the following model for fracture-controlled fluid circulation and associated dissolutional weathering of carbonate rocks (Fig. 7). Meteoric H_2O–CO_2 solutions infiltrate from the surface through the fractured carbonate strata (e.g. Dreybrodt, 1988; White, 1988; Ford and Williams, 1989; Agosta and Kirschner, 2003). Joints, bedding surfaces, and fault damage zones are preferential pathways for the infiltrating solutions. The acidic properties of such solutions and the contrast of permeability between the fault damage zones and the surrounding jointed carbonate strata (e.g. Caine et al., 1996; Evans et al., 1997; Agosta et al., in press) are at the origin of two different modes of dissolutional weathering: (i) a mode of diffuse weathering, consisting in the karstification of bedding surfaces and of closely spaced joints. This mode of dissolutional weathering affects only the strata shallower than ~5 m, because through these shallow strata the infiltrating solutions lose most of their acidic properties and,

Table 1
Results from stable isotope analyses

Sample	Rock type	Depth (m)	Fault kinematics	$\delta^{18}O$	$\delta^{13}C$
CRN1a	Limestone (host rock)	~45		28.99	2.46
CRN1b	Limestone (host rock)	~45		28.99	2.41
CRN1c	Calcite concretion	~45	Strike-slip	25.14	−4.66
CRN1d	Calcite concretion	~45	Strike-slip	25.02	−4.58
CRN2a	Calcite concretion	~45	Strike-slip	24.87	−6.74
CRN2b	Calcite concretion	~45	Strike-slip	25.49	−10.90
CRN3a	Limestone (host rock)	~45		29.26	2.55
CRN4a	Limestone (host rock)	~45		28.76	2.02
CRN4b	Limestone (host rock)	~45		28.83	2.14
CRN5a	Limestone (host rock)	~55		28.88	2.37
CRN5b	Calcite concretion	~55	Strike-slip	25.67	−7.06
CRN5c	Calcite concretion	~55	Strike-slip	25.33	−8.82
CRN6a	Calcite concretion	~55	Strike-slip	26.20	−8.55
CRN6b	Calcite concretion	~55	Strike-slip	26.34	−7.34
CRN7a	Limestone (host rock)	~55		28.39	2.55
CRN7b	Calcite concretion	~55	Strike-slip	26.17	−8.68
CRN7c	Calcite concretion	~55	Strike-slip	26.07	−9.37
CRN8a	Limestone (host rock)	~55		28.68	2.76
CRN9a	Limestone (host rock)	~55		28.49	2.23
CRN10a	Calcite concretion	~35	Transtensional	25.00	−3.48
CRN10b	Calcite concretion	~35	Transtensional	24.81	−3.89
CRN11a	Calcite concretion	~35	Transtensional	25.66	−7.30
CRN12a	Limestone (host rock)	~35		29.49	1.29
CRN12b	Limestone (host rock)	~35		29.70	1.51
CRN13a	Limestone (host rock)	~35		28.91	3.00

The host rock consists of limestones from the Calcare Massiccio Formation. The calcite concretions are deposited over the fault surfaces or within the associated damage zones. Depths are from the fieldsurface. See Fig. 2 for sample location.

therefore, their $CaCO_3$-dissolutional capability at deeper levels. This process is probably controlled by a low velocity of permeation and, therefore, a relatively long-lasting fluid-rock interaction at shallow levels. The difference in the density correlations (joints vs. karstic cavities, Fig. 5b and c) observed for the Calcare Massiccio Formation and for the Maiolica Formation should be ascribed to the difference in lithology and, therefore, in the aptitude of being dissolved. The Maiolica Formation is, in fact, often dolomitized, whereas the Calcare Massiccio Formation usually consists of nearly pure limestone; (ii) a mode of more concentrated weathering occurring within fault damage zones, whose high permeability (e.g. Caine et al., 1996) causes a rapid infiltration of meteoric waters and, therefore, a fluid–rock interaction briefer than that occurring in the surrounding jointed rocks. It follows that the effects of the dissolutional weathering along the fault damage zones can be observed even at depths of about 70 m, where the dissolutional enlargement of joints and bedding

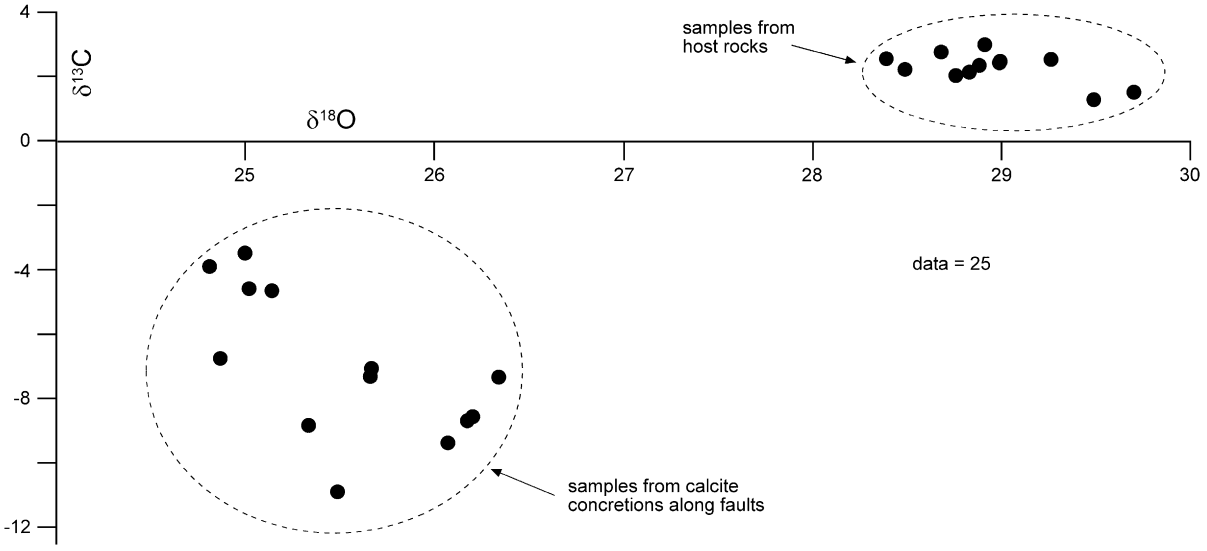

Fig. 6. Relationship between $\delta^{18}O$ and $\delta^{13}C$ for calcite concretions collected along a few faults and for samples of the relative host rock (i.e. limestone from the Calcare Massiccio Formation). The relative values are listed in Table 1.

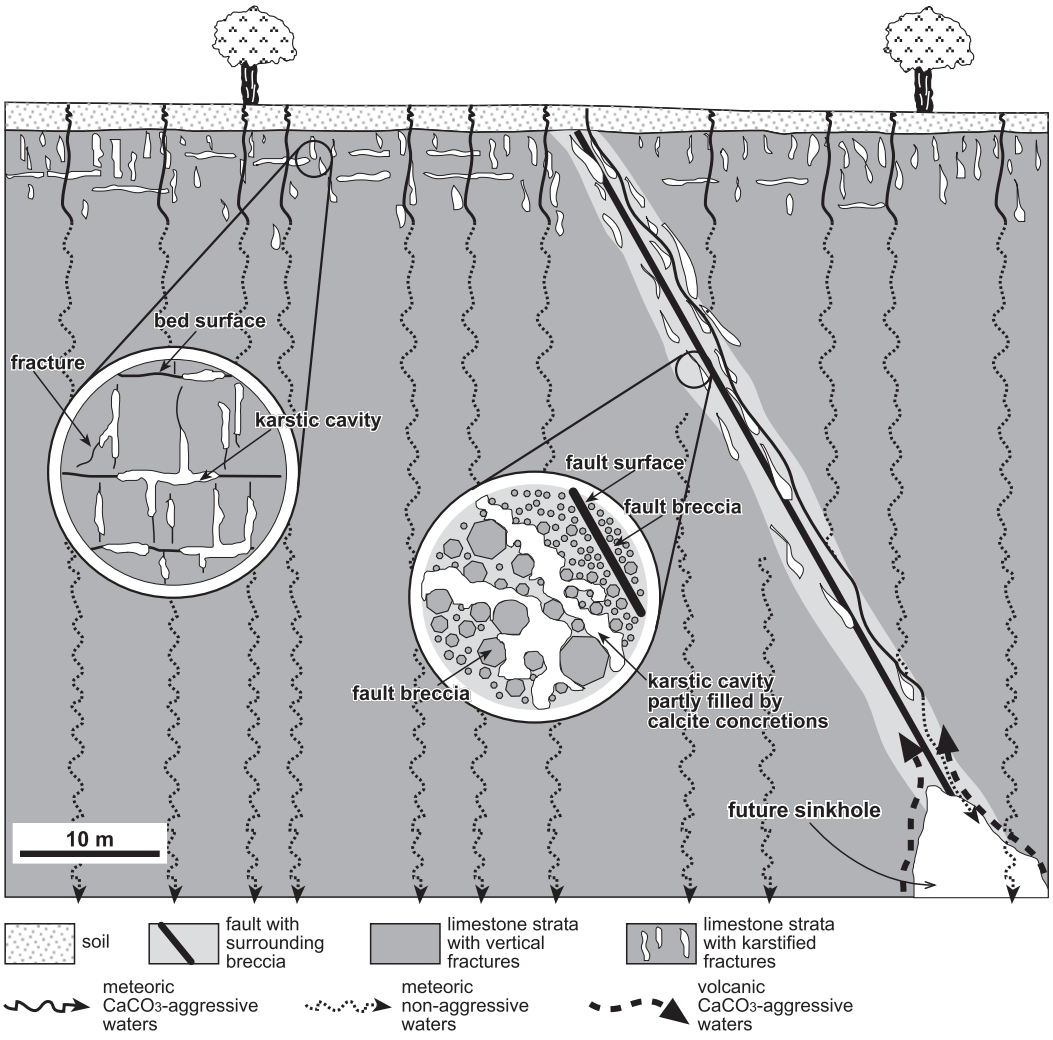

Fig. 7. Model for structurally controlled fluid circulation in carbonate strata and related development of dissolutional cavities. Insets show details from the fault damage zone and from the jointed host rock.

surfaces in the surrounding rocks is absent. As above-discussed, some stable isotope data suggest that the dissolutional weathering of fault damage zones may also be connected with the outflow of volcanic waters. In particular, such a dissolutional weathering may be the result of a mixing corrosion caused by the interaction between meteoric and volcanic waters at hypogeal levels (e.g. Gabrovšek and Dreybrodt, 2000; Kaufmann, 2003b; Romanov et al., 2003). This process may be the cause for the deep cave and sinkhole system in the Cornicolani Mountains region. The causal connection between hypogeal karstification of limestone and volcanic activity has been established in several other sites on the Earth (e.g. Bakalowicz et al., 1987; Gary et al., 2002).

5. Conclusions

(1) The fluid circulation through the carbonate strata of the Cornicolani Mountains and the associated dissolutional weathering is controlled by the fracture pattern. This is demonstrated by the presented relationships between fractures and the associated karstic cavities (Fig. 5). These relationships are here quantified for the first time by using field-based data.

(2) The pattern of fractures and associated karstic structures (Figs. 3–5) shows that the dissolutional weathering of jointed carbonate strata consists of a downward erosion by meteoric waters (Fig. 6). This process is significantly shallower than the dissolutional weathering of fault damage zones (Fig. 4), along which upward erosion by volcanic waters can possibly occur (Fig. 6).

(3) From the analysis of karstic structures (e.g. Fig. 4d) and from some stable isotope data (Fig. 6) it is inferred that the sinkhole-related hazard is much greater along the fault zones than in the surrounding fractured rocks. To mitigate such hazards, the fault zones should be defined, characterized, and monitored also when blanketed by recent deposits. In particular, the structural architecture and permeability of faults as well as the variability of these parameters along both strike and dip of faults should be carefully addressed to infer the preferential pathways of fluids.

Acknowledgments

We thank D. Cosentino for sharing with us unpublished results from detailed geological mapping of the Cornicolani Mountains and F. Salvini for providing the DAISY software for structural analysis. F. Agosta and an anonymous reviewer are thanked for their constructive comments. C. Passchier is thanked for the editorial work.

References

Agosta, F., Kirschner, D.L., 2003. Fluid conduits in carbonate-hosted seismogenic normal faults of central Italy. Journal of Geophysical Research 108, 2221, doi:10.1029/2002JB002013.

Agosta, F., Prasad, M., Aydin, A. Physical properties of carbonate fault rocks, Fucino basin, central Italy: implications for fault seal in platform carbonates. Geofluids, in press.

Alfonsi, L., Funiciello, R., Girotti, O., Mattei, M., Maiorani, A., Preite Martinez, M., Trudu, C., Turi, B., 1991. Structural and geochemical features of the Sabina strike-slip fault (central Apennines). Bollettino della Società Geologica Italiana 110, 217–230.

Andre, B.J., Rajaram, H., 2005. Dissolution of limestone fractures by cooling waters: early development of hypogene karst systems. Water Resources Research 41, W01015, doi:10.1029/2004WR003331.

Bakalowicz, M.J., Ford, D.C., Miller, T.E., Palmer, A.N., Palmer, M.V., 1987. Thermal genesis of dissolution caves in the Black Hills, South Dakota. Geological Society of America Bulletin 99, 729–738.

Baker, A., Ito, E., Smart, P.L., McEwan, R.F., 1997. Elevated and variable values of $\delta^{13}C$ in speleothems in a British cave system. Chemical Geology 136, 263–270.

Bauer, S., Liedl, R., Sauter, M., 2000. Modelling of karst development considering conduit matrix exchange flow. In: Stauffer, F., Kinzelbach, W., Kovar, K., Hoehn, E. (Eds.), Calibration and Reliability in Ground Water Modelling. IAHS Publication 265, 10–15.

Caine, J.S., Evans, J.P., Forster, C.B., 1996. Fault zone architecture and permeability structure. Geology 24, 1025–1028.

Caramanna, G., 2002. Exploring on of the world's deepest sinkholes: the Pozzo del Merro (Italy). Underwater Speleology February, 4–8.

Cavinato, G., DeCelles, P.G., 1999. Extensional basins in tectonically bimodal central Apennines fold-thrust belt, Italy: response to corner flow above a subducting slab in retrograde motion. Geology 27, 955–958.

Cipollari, P., Cosentino, D., 1991. La linea Olevano-Antrodoco: contributo della biostratigrafia alla sua caratterizzazione cinematica. Studi Geologici Camerti 2, 143–149.

Cipollari, P., Cosentino, D., 1995. Miocene unconformities in the central Apennines: geodynamic significance and sedimentary basin evolution. Tectonophysics 252, 375–389.

Chiocchini, M., Manganelli, V., Pannunzi, L., 1979. Ricerche geologiche sul Mesozoico della Sabina (Lazio). II. I Monti Cornicolani. Bollettino del Servizio Geologico d'Italia 100, 235–264.

Clemens, T., Huckinghaus, D., Liedl, R., Sauter, M., 1999. Simulation of the development of karst aquifers: role of the epikarst. International Journal of Earth Sciences 88, 157–162.

Colombi, A., 2002. Sinkhole nel Lazio: nuovi orizzonti? Professione Geologo 1, 14–16.

Cosentino, D., Cipollari, P., Pasquali, V., 2004. The Jurassic pelagic carbonate platform of the Cornicolani Mountains. (Central Apennines). In: Pasquarè, G., Venturin, C. (Eds.), Mapping Geology in Italy. APAT, Rome, pp. 177–184.

Davis, G.H., Reynolds, S.J., 1996. Structural Geology of Rocks and Regions. Wiley, New York.

Dewey, J.F., Helman, M.L., Turco, E., Hutton, D.H.W., Knott, S.D., 1989. Kinematics of the western Mediterranean. In: Coward, M.P., Dietrich, D., Park, R.G. (Eds.), Alpine Tectonics. Geological Society, London, Special Publications, vol. 45, pp. 265–283.

Dreybrodt, W., 1980. Deposition of calcite from thin films of calcareous solution and growth of speleothems. Chemical Geology 29, 89–105.

Dreybrodt, W., 1988. Processes in Karst Systems – Physics, Chemistry and Geology. Springer, Berlin.

Dreybrodt, W., 1996. Principles of early development of karst conduits under natural and man-made conditions revealed by mathematical analysis of numerical models. Water Resources Research 32, 2923–2935.

Evans, J.P., Forster, C.B., Goddard, J.V., 1997. Permeability of fault-related rocks, and implications for hydraulic structure of fault zones. Journal of Structural Geology 19, 1393–1404.

Faccenna, C., Florindo, F., Funiciello, R., Lombardi, S., 1993. Tectonic setting and sinkholes features: case histories from western central Italy. Quaternary Proceedings 3, 47–57.

Faccenna, C., Funiciello, R., 1993. Tettonica pleistocenica tra il Monte Soratte e I Monti Cornicolani (Lazio). Il Quaternario 6, 103–118.

Faccenna, C., Funiciello, R., Montone, P., Parotto, M., Voltaggio, M., 1994. Late Pleistocene strike-slip tectonics in the Acque Albule Basin (Tivoli, Latium). Memorie Descrittive della Carta Geologica d'Italia 49, 37–50.

Fetter, C.W., 1980. Applied Hydrogeology. Merrill Publishing, Columbus, Ohio.

Ford, D.C., Ewers, R.O., 1978. The development of limestone caves in the dimensions of length and depth. Canadian Journal of Earth Sciences 15, 1783–1798.

Ford, D.C., Williams, P.W., 1989. Karst Geomorphology and Hydrology. Unwin Hyman, London.

Funiciello, R., Giordano, G., De Rita, D., 2003. The Albano maar lake (Colli Albani Volcano, Italy): recent volcanic activity and evidence of pre-Roman Age catastrophic lahar events. Journal of Volcanology and Geothermal Research 123, 43–61.

Gabrovšek, F., 2000. Evolution of Early Karst Aquifers: From Simple Principles to Complex Models. Zalozba ZRC, Ljubljana.

Gabrovšek, F., Dreybrodt, W., 2000. The role of mixing corrosion in calcite aggressive $H_2O–CO_2–CaCO_3$ solutions in the early evolution of karst aquifers. Water Resources Research 36, 1179–1188.

Gabrovšek, F., Dreybrodt, W., 2001. A model of the early evolution of karst aquifers in limestone in the dimensions of length and depth. Journal of Hydrology 240, 206–224.

Gabrovšek, F., Romanov, D., Dreybrodt, W., 2004. Early karstification in a dual-fracture aquifer: the role of exchange flow between prominent fractures and a dense net of fissures. Journal of Hydrology 299, 45–66.

Gary, M.O., Sharp, J.M., Havens, R.S., Stone, W.C., 2002. Sistema Zacatón: identifying the connection between volcanic activity and hypogenic karst in a hydrothermal phreatic cave system. Geo2 29, 1–14.

Gary, M.O., Sharp, J.M., Caramanna, G., Havens, R.S., 2003. Volcanically influenced speleogenesis: forming El Sistema Zacatón, Mexico, and Pozzo Merro, Italy, the deepest phreatic sinkholes in the world. Geological Society of America Abstracts with Programs 35, 52.

Gascoyne, M., 1992. Palaeoclimate determination from cave calcite deposits. Quaternary Science Reviews 11, 609–632.

Ghisetti, F., Kirschner, D.L., Vezzani, L., Agosta, F., 2001. Stable isotope evidence for contrasting paleofluid circulation in thrust faults and normal faults of the central Apennines, Italy. Journal of Geophysical Research 106, 8811–8826.

Hendy, C.H., 1971. The isotopic geochemistry of speleothems. 1. The calculation of the effects of the different modes of formation on the isotopic composition of speleothems and their applicability as palaeoclimatic indicators. Geochimica et Cosmochimica Acta 35, 801–824.

Kaufmann, G., 2002. Karst aquifer evolution in a changing watertable environment. Water Resources Research 38, 261–269.

Kaufmann, G., 2003a. A model comparison of karst aquifer evolution for different matrix-flow formulations. Journal of Hydrology 283, 281–289.

Kaufmann, G., 2003b. Numerical models for mixing corrosion in natural and artificial karst environments. Water Resources Research 39, 1157, doi:10.1029/2002WR001707.

Kaufmann, G., Braun, J., 1999. Karst aquifer evolution in fractured, porous rocks. Water Resources Research 35, 3223–3238.

Kaufmann, G., Braun, J., 2000. Karst aquifer evolution in fractured rocks. Water Resources Research 36, 1381–1391.

Knab, O., 2003. Die tiefsten Unterwasserhöhlen der Welt. Höhlenpost Stand 121, 32–33.

Maiorani, A., Funiciello, R., Mattei, M., Turi, B., 1992. Stable isotope geochemistry and structural elements of the Sabina region (Central Apennines, Italy). Terra Nova 4, 484–488.

Malinverno, A., Ryan, W.B.F., 1986. Extension in the Tyrrhenian Sea and shortening in the Apennines as result of arc migration driven by sinking of the lithosphere. Tectonics 5, 227–245.

McDermott, F., 2004. Palaeo-climate reconstruction from stable isotope variations in speleothems: a review. Quaternary Science Reviews 23, 901–918.

Minissale, A., Evans, W.C., Magro, G., Vaselli, O., 1997. Multiple source components in gas manifestations from north-central Italy. Chemical Geology 142, 175–192.

Minissale, A., Kerrick, D.M., Magro, G., Murrell, M.T., Paladini, M., Rihs, S., Sturchio, N.C., Tassi, F., Vaselli, O., 2002. Geochemistry of Quaternary travertines in the region north of Rome (Italy): structural, hydrologic and paleoclimatic implications. Earth and Planetary Science Letters 203, 709–728.

O'Neil, J.R., Clayton, R.N., Mayeda, T.K., 1969. Oxygen isotope fractionation in divalent metal carbonates. Journal of Chemical Physics 51, 5547–5558.

Palmer, A.N., 1991. The origin and morphology of limestone caves. Geological Society of America Bulletin 103, 1–21.

Passeri, L., 1972. Ricerche sulla porosità delle rocce carbonatiche nella zona di M.te Cucco (Appennino Umbro-Marchigiano) in relazione alla genesi della canalizzazione interna. Le Grotte d'Italia 4, 5–55.

Patacca, E., Sartori, R., Scandone, P., 1992. Tyrrhenian basin and Apenninic arcs: kinematic relations since late Tortonian times. Memorie della Società Geologica Italiana 45, 425–451.

Rodet, J., 1999. Le réseau de fracturation, facteur initial de la karstification des craies dans le collines du Perche: l'example du site de la Mansonnière (Bellou-sur-Huisne, Orne, France). Geodinamica Acta 12, 259–265.

Romanov, D., Gabrovšek, F., Dreybrodt, W., 2003. The impact of hydrochemical boundary conditions on the evolution of limestone karst aquifers. Journal of Hydrology 276, 240–253.

Salomons, W., Mook, W.G., 1986. Isotope geochemistry of carbonates in the weathering zone. In: Fritz, P., Fontes, C.J. (Eds.), The Terrestrial Environment, B. Handbook of Environmental Isotope Geochemistry, vol. 2. Elsevier, Amsterdam, pp. 239–270.

Salvati, R., Sasowsky, I.D., 2002. Development of collapse sinkhole in areas of groundwater discharge. Journal of Hydrology 264, 1–11.

Salvini, F., Billi, A., Wise, D.U., 1999. Strike-slip fault-propagation cleavage in carbonate rocks: the Mattinata Fault zone. Journal of Structural Geology 21, 1731–1749.

Schwarcz, H.P., 1986. Geochronology and isotopic geochemistry of speleothems. In: Fritz, P., Fontes, J.Ch. (Eds.), The Terrestrial Environment, B. Handbook of Environmental Isotope Geochemistry, vol. 2. Elsevier, Amsterdam, pp. 271–303.

Sowers, G.F., 1996. Building on Sinkholes. American Society of Civil Engineers, New York.

Sweeting, M.M., 1950. Erosion cycles and limestone caverns in the Ingleborough District (England). Journal of Geology 115, 63–78.

Swinnerton, A.C., 1932. Origin of limestone caverns. Geological Society of America Bulletin 34, 662–693.

Titley, S.R., 1976. Evidence for a Mesozoic linear tectonic pattern in southeastern Arizona. Arizona Geological Society Digest 10, 71–101.

Veizer, J., Hoefs, J., 1976. The nature of $^{18}O/^{16}O$ and $^{13}C/^{12}C$ secular trends in sedimentary carbonate rocks. Geochimica et Cosmochimica Acta 40, 1387–1395.

White, W.B., 1988. Geomorphology and Hydrology of Karst Terrains. Oxford University Press, Oxford.

White, W.B., 2002. Karst hydrology: recent developments and open questions. Engineering Geology 65, 85–105.